Pergamon

Chemical Engineering Science, Vol. 52, No. 12, pp. 1861–1874, 1997

Printed in Great Britain

PII: S0009-2509(96)00518-0

0009-2509/97 $17.00 + 0.00

Dispersion in periodic porous media. Experience versus theory for two-dimensional systems

Sophie Didierjean,* Helio Pedro Amaral Souto,† Renaud Delannay* and Christian Moyne*

* Laboratoire d'Energétique et de Mécanique Théorique et Appliquée, URA CNRS 875, Institut National Polytechnique de Lorraine – Université Henri Poincaré, 2, avenue de la Forêt de haye, 54504 Vandœuvre Cedex, France; † Instituto Politécnico – UERJ, Caixa Postal 97282 Nova Friburgo, RJ Cep 28601-970, Brazil

(Received 8 January 1996; accepted 4 December 1996)

Abstract—A method is presented for the experimental study of dispersion in saturated porous media for two-dimensional spatially periodic systems. The use of stereophotolithography laser as the basis of the porous media fabrication process made this investigation feasible. The porous media consist of a set of circular cylinders accurately positioned in an ordered (in line) or in a disordered (random) unit cell periodically reproduced in the plane of the study. For two directions of the average fluid velocity in the in-line array and one direction of the velocity vector in the disordered array, dye is injected in the form of a pulse at the entrance to the medium. The tracer concentration variations with time are measured by a video camera and are averaged over a unit cell. The measured time distributions are compared with computations using the macroscopic convection–diffusion equation in order to estimate the longitudinal dispersion coefficient. The variations of this coefficient with particulate Péclet number in the three geometries investigated are compared with the available numerical results. All the results agree, showing a significant influence of the direction of the average fluid velocity for the ordered medium. Concerning the random medium, the results appear to indicate that, in spite of its periodic character, this type of medium is capable of describing the behaviour of disordered porous media. This original technique is highly promising for the explanation of dispersion mechanisms in porous media.

INTRODUCTION

This paper investigates dispersion due to macroscopic spreading of a neutrally buoyant solute introduced into a fluid flowing through a saturated spatially periodic porous medium. This spreading is the result of the combined effects of Brownian motion (molecular diffusion) and local variations of the interstitial velocity (due to the position of the solid boundaries).

In spatially periodic media, the determination of dispersion properties is reduced to a resolution in a single unit cell. This attractive characteristic was first pointed out by Brenner (1980), who used the method of spatial moments introduced by Aris (1956) and extended by Horn (1971) to obtain the asymptotic behaviour of long-time distribution of a solute injected into a porous medium. The solute concentration then obeys the usual convection–diffusion equation at the macroscopic scale. Other authors have developed concurrent theories: Carbonell and Whitaker (1983) used the volume-averaging technique to obtain a complete expression for the dispersion tensor, including an antisymmetric part (which of course plays no role in the macroscopic convection–diffusion equation). The method of 'configurational' averaging over a set of media is used by Koch *et al.* (1985). Another technique is the homogenization method as proposed by Rubinstein and Mauri (1986) and Mei (1992).

All these theories agree in their conclusions: the long-time behaviour of a solute transported through a spatially periodic porous medium is described on the macroscopic scale by a convection–diffusion equation. The macroscopic dispersion coefficient can be calculated by solving a closure problem on the unit cell. This equation, as well as the flow equations, are generally solved numerically. The solution is obtained using the finite-element method by Eidsath *et al.* (1983), and Edwards *et al.* (1991), the finite-volume method, as used by Amaral Souto (1993), and the finite-difference method used by Salles *et al.* (1993). In the latter work, the dispersion tensor is also evaluated by a random walk method. However, using a number of simplifying assumptions, Koch *et al.* (1989)

obtained analytical solutions for periodic beds of low solid fraction. They predicted a functional dependence of the diffusivity on the Péclet number, which is not in agreement with the previous numerical results. On the other hand, few experiments have been performed on periodic porous media. To our knowledge, only Gunn and Pryce (1969) have published results on regular arrangements of spherical particles.

This paper helps to meet the need for more experimental data on periodic media. These data are needed to test the validity of the various approaches used and, more specifically, to help to clarify the conflicting results previously reported. The following section offers a brief theoretical analysis. Experimental procedures and results are examined in the two next sections, respectively. The experimental measurements are then compared with the numerical calculations of Amaral-Souto (1993), followed by a general discussion.

THEORY

The long-time behaviour of solute transport through a spatially periodic porous medium is described on the macroscopic scale by a convection–diffusion equation. The macroscopic dispersion tensor can be calculated by solving a closure problem on the unit cell. A brief review of the theory is given below, following the volume-average method. As pointed out by Baveye and Sposito (1984), a link exists between the definition of the averaged quantities and the experimental measuring device. Since the experimental technique uses image processing, the weighting function applied to the concentration measurement for the fluid volume, V_f, inside the measurement volume, V, is the fluid characteristic function (which is 1 in the fluid, 0 elsewhere). If c denotes the solute volume concentration, the intrinsic average concentration $\langle c\rangle^f$ is defined as

$$\langle c\rangle^f = \frac{1}{V_f}\int_{V_f} c\,\mathrm{d}V. \tag{1}$$

The equation governing convective and diffusive transport at the pore level is

$$\frac{\partial c}{\partial t} + \mathbf{v}\cdot\nabla c = \nabla\cdot(\mathscr{D}\nabla c) \tag{2}$$

where $\mathscr{D}$ is the molecular diffusion coefficient. The fluid is assumed to be incompressible.

Since the solid is impervious to the solute, the boundary condition on the surface A_{fs} between the solid (s) and fluid (f) phases is thus

$$\mathbf{n}\cdot\nabla c = 0 \tag{3}$$

where $\mathbf{n}$ is the external normal to the fluid phase on the fluid–solid interface A_{fs}.

Assuming a quasi-steady closure of the problem, the average transport equation is given by (Carbonell and Whitaker, 1983)

$$\frac{\partial\langle c\rangle^f}{\partial t} + \langle\mathbf{v}\rangle^f\cdot\nabla\langle c\rangle^f = \mathbf{D}^*:\nabla\nabla\langle c\rangle^f. \tag{4}$$

The dispersion tensor $\mathbf{D}^*$ is the sum of three parts

$$\mathbf{D}^* = \mathscr{D}(\mathbf{I} + \tau) + \mathbf{D} \tag{5}$$

where $\mathbf{I}$ is the unit tensor. The tortuosity tensor τ is defined by

$$\tau = \frac{1}{V_f}\int_{A_{fs}} \mathbf{n}\mathbf{f}\,\mathrm{d}A \tag{6}$$

whereas the hydrodynamic dispersion tensor $\mathbf{D}$ is written

$$\mathbf{D} = \frac{1}{V_f}\int_{V_f} \tilde{\mathbf{v}}\mathbf{f}\,\mathrm{d}A \tag{7}$$

where $\tilde{\mathbf{v}} = \mathbf{v} - \langle\mathbf{v}\rangle^f$ is the spatial fluctuation of the velocity field. The vector $\mathbf{f}$ is the solution of the closure equation

$$\mathbf{v}\cdot\nabla\mathbf{f} = \mathscr{D}\nabla^2\mathbf{f} - \tilde{\mathbf{v}}. \tag{8}$$

The boundary condition on the interface A_{fs} is expressed:

$$-\mathbf{n}\cdot\nabla\mathbf{f} = \mathbf{n}. \tag{9}$$

For a spatially periodic porous medium, since the average on the volume of a unit cell is assumed to coincide with the average on a 'representative elementary volume', the volume V is taken as a unit cell of the medium. On the external surface of the unit cell, A_{fe}, periodicity boundary conditions are used for the function $\mathbf{f}$:

$$\mathbf{f}(\mathbf{r} + \mathbf{l}_i) = \mathbf{f}(\mathbf{r}) \tag{10}$$

$$\mathbf{n}\cdot\nabla\mathbf{f}(\mathbf{r} + \mathbf{l}_i) = \mathbf{n}\cdot\nabla\mathbf{f}(\mathbf{r}) \tag{11}$$

where $\mathbf{r}$ is the spatial position of a point inside the unit cell, $\mathbf{l}_i$ ($i = 1, 2$) the lattice vectors of the unit cell, and $\mathbf{n}$ is the normal to the unit cell.

The finite-volume method is the numerical method used to solve the closure equation. Special care was taken to avoid numerical dispersion, which is of course an undesirable effect and can, if not prevented, distort the results for the dispersion tensor. The details are given elsewhere by Amaral Souto (1993), and Amaral Souto and Moyne (1996b).

EXPERIMENTAL DESIGN AND PROCEDURE

The main objective of this study is to describe the macroscopic spreading of a passive solute by observing the phenomena at the microscopic pore level for a periodic medium. The experimental results are compared with the mathematical description of the process going from the local equation (2) to the average version (4).

Experiments are much easier to conduct on two-dimensional systems. The transparency of the system makes possible to observe the concentration field

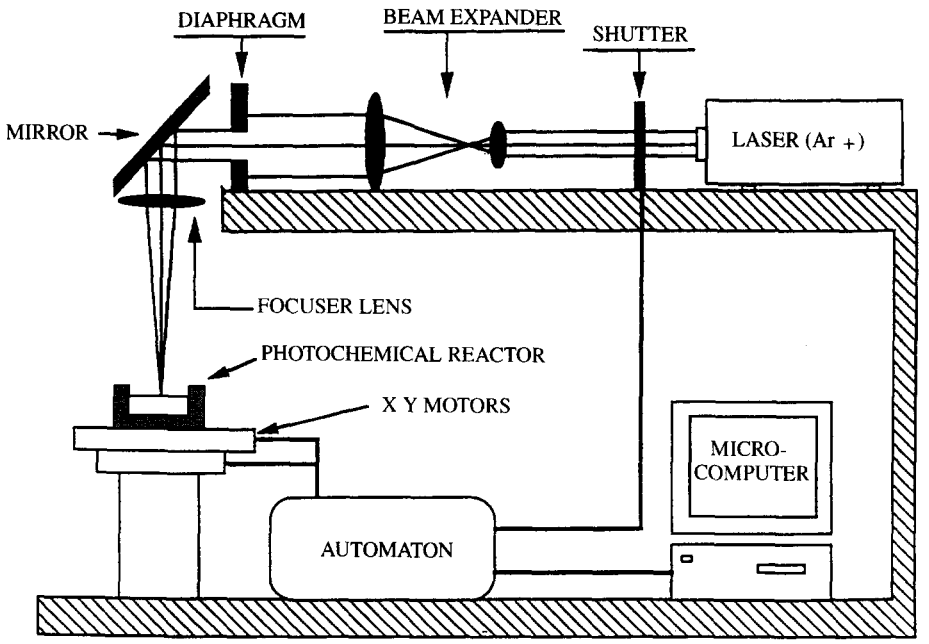

Porous media fabrication; experimental set-up.

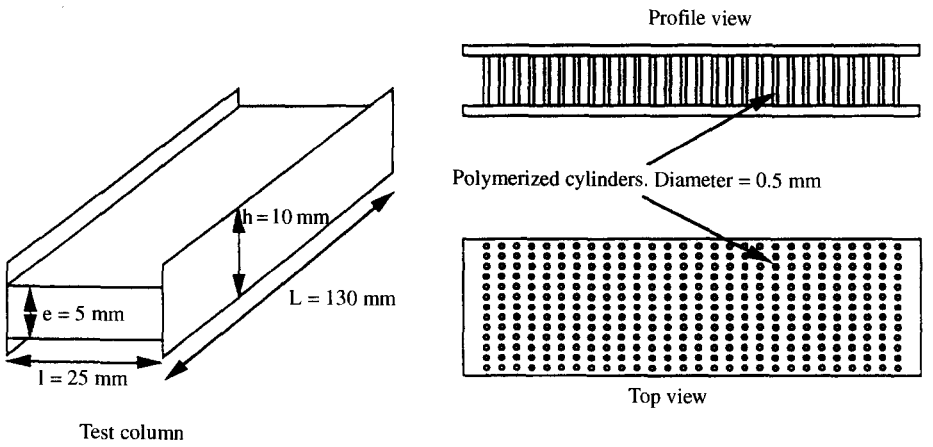

Polymerized cylinders and test-column.

Fig. 1. Manufacture of porous media: experimental set-up.

directly. On the other hand, numerical results are available in two dimensions but are scarce in three dimensions.

Manufacturing the porous media

In order to study dispersion through periodic media, the first task is to build a spatially periodic medium with a good geometric definition. Laser stereophotolithography (SPL) seems to be an attractive way of doing this. SPL is based on a liquid–solid transformation of a photosensitive substance (acrylate monomer) by laser action. Objects of complex structure can be manufactured with a computer-controlled incident beam as reported by André and Corbel (1994), Karrer *et al.* (1992) and Corbel *et al.* (1994).

The porous media consist of any repetitive array of cylinders fixed between two glass plates. The cylinders here are circular, with a diameter of about 5×10^{-4} m and a height of about 5×10^{-3} m. The experimental set-up is shown in Fig. 1. The array geometry is stored in a microcomputer which drives the programmable controller which performs two functions. The first is to drive the photochemical reactor with two step-by-step motors in a plane perpendicular to the laser beam, with an accuracy of 10 μm. The second is to activate the UV laser shutter. To obtain a shape as perfect as possible, the various parameters of the SPL process (chemical composition of the mixture, light power, exposure time) are optimized. A beam expander associated with a diaphragm evens out the laser's

Gaussian energy distribution into a near-uniform distribution. At the end of the process, the excess monomer is drained off, which is a difficult operation because of the monomer's high viscosity. A typical medium comprises about 4000 cylinders (140 in the direction of mean flow and 30 in the direction perpendicular to it). Three arrangements of particles in the unit cell were investigated: in-line cylinders, with an axis of symmetry parallel to the average flow direction [Fig. 2(a)]; the same geometry rotated 26° [Fig. 2(b)]; and a third medium [Fig. 2(c)] of a randomly distributed unit cell reproduced periodically in the plane of study. The cylinder location in the unit cell is given by a random number generator.

Concentration measurements

Among various tracers, methylene blue dye in water (for which no adsorption with the solid phase was observed) was selected for this study. Since image processing is used, a precise relationship is needed between the grey level measured by the camera and the volume concentration of methylene blue dye. According to Beer–Lambert, the transmission coefficient for a monochromatic beam of wavelength λ through an absorbent material of thickness x is given by

$$\tau_\lambda = \exp(-\alpha_\lambda x) \tag{12}$$

where α_λ is the absorption coefficient of the material for the wavelength λ. If the material is a dye of low

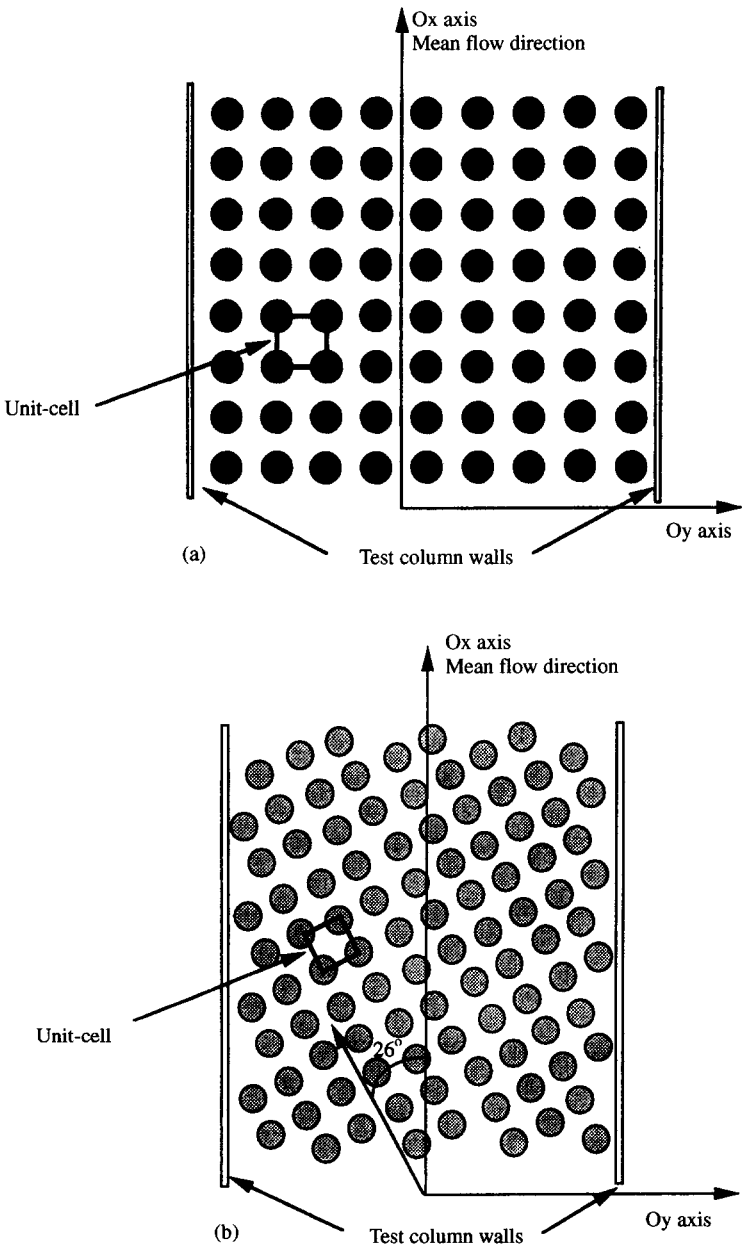

Fig. 2. (a) In-line cylinders. Mean flow at 0°. (b) In-line cylinders. Mean flow at 26°. (c) Random distributed medium. Mean flow at 0°.

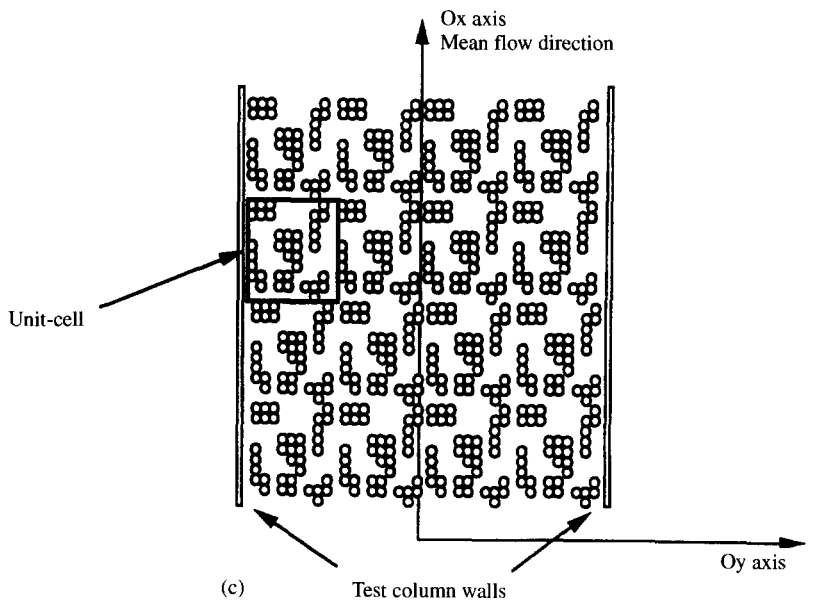

Fig. 2. (*Continued*).

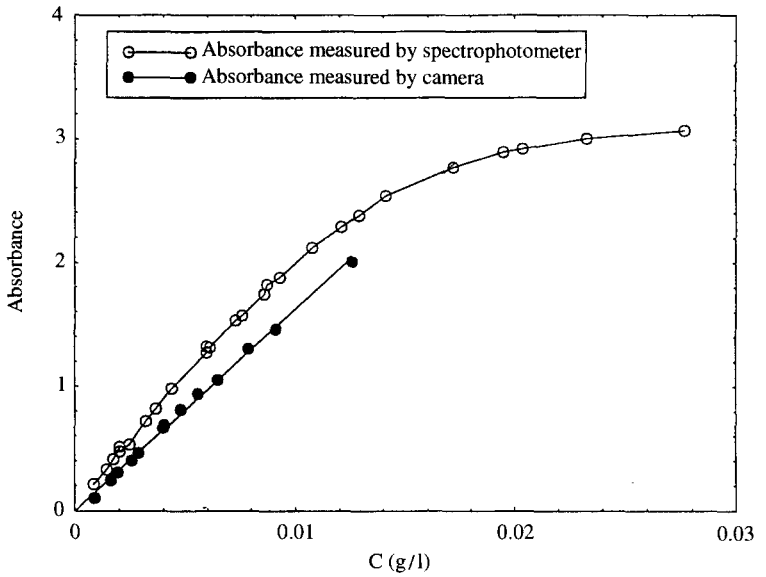

Fig. 3. Comparison between absorbances measured with a spectrophotometer and by video camera.

concentration c dissolved in a non-absorbent material, then

$$\alpha_\lambda = \varepsilon_\lambda c \tag{13}$$

where ε_λ is the molecular extinction coefficient, a function of λ. The wavelength for maximum dye absorption was determined by using a spectrophotometer at $\lambda_{max} = 664$ nm. A band passfilter (650–660 nm) was therefore used. The light source was a white light source. The detector was a CCD video camera generating a signal proportional to the light intensity. The analogic signal given by the camera was converted by A/D converter and analysed by a computer using the Visilog image processor. This made it possible to access the value of the grey level on the image coded on 8 bits giving 256 grey levels. The absorbance ($\varepsilon_\lambda cx$) of the solution vs the concentration c measured with the spectrophotometer is plotted in Fig. 3 for $\lambda = \lambda_{max}$. Since the camera signal is proportional to the light intensity, it seems reasonable to try to use the same type of equation as eq. (12) for the grey levels:

$$N = N_0 \exp(-\varepsilon cx) \tag{14}$$

where N_0 is the grey level measured with no solute. Clearly, the relation $\ln(N_0/N)$ vs c shown in Fig. 3 demonstrates the validity of the above assumptions

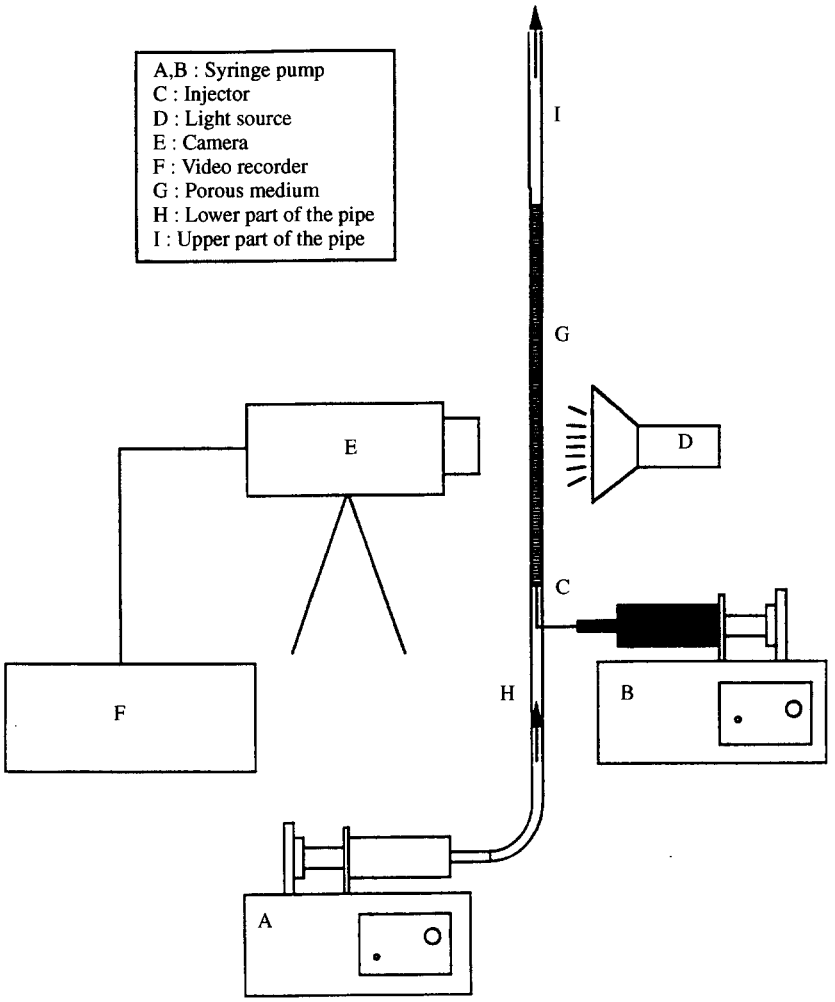

Fig. 4. Experimental system for concentration measurements.

with a correlation coefficient of 0.98. To conclude this section, for concentrations of less than 0.01 g/l, the relation $\ln(N_0/N)$ vs c is linear.

Experimental method

The experimental set-up is shown in Fig. 4. The porous medium manufactured by SPL is placed between two pipes having the same rectangular cross-section. Water is driven through the medium by a syringe pump designed to obtain a constant flow rate in the range 4×10^{-9} to 4×10^{-8} m^3/s. Although the dye concentration is small, the column is placed vertically and the flow is straight upward to minimize natural convection. A small volume of dye solution (about 20 µl) is injected into the stopped flow at the medium entrance by a small needle located at the centre of the flow. To control the amount of dye injected, the needle is connected to another syringe pump. At $t = 0$ the dye is injected for a short period of time, forming a pulse both in time and in space. The camera is in-line with a video tape recorder whose recording frequency is 25 Hz. For good resolution, a macroscopic lens is placed on the video camera. Figure 5 shows an image of the dispersing dye through a random distributed array. The images are processed in order to measure the dye concentration as a function of space and time.

Intrinsic mean concentration

For this study, it was decided to determine the intrinsic average dye concentration over a unit cell of the periodic medium according to eq. (1), where V_f is the fluid volume in a unit cell of the medium. A threshold is established on the basis of an image of the empty medium, in order to construct a binary image of the medium in which 0 stands for solid-phase pixels and 1 for fluid-phase pixels. A histogram of this binary image provides a simple measure of the medium porosity. To obtain the intrinsic mean concentration, the grey-level image of the process is multiplied by the binary image of the medium, and only then are the non-zero grey levels of the unit cell taken into account. At each point, the concentration is determined by the Beer–Lambert law (14). This value is then averaged over the unit cell and assigned to the centre point of the unit cell, denoted $\langle c \rangle_{\text{cell}}$. For example, Figs 6–9 show the average dye concentration over a unit cell for various experiments. Due to the

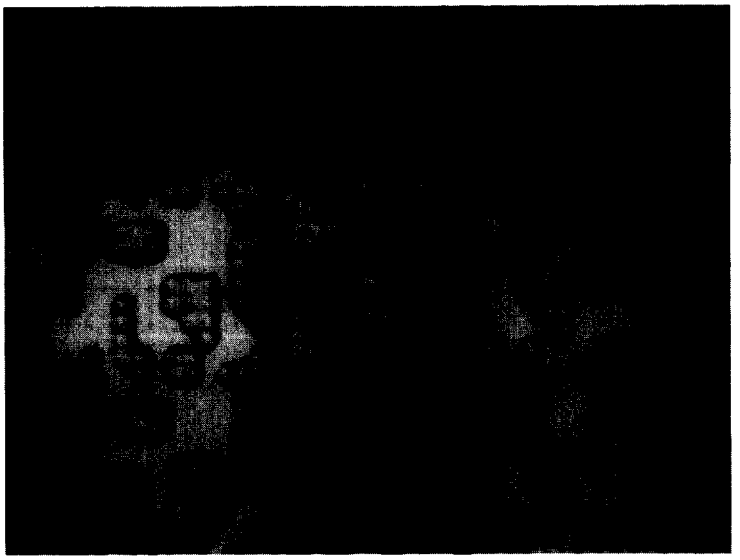

Fig. 5. Image of the dispersion process in a random distributed medium.

averaging process, the measurement noise appears to be rather low.

Longitudinal dispersion coefficient measurement

For dispersion in two-dimensional porous media, the change in mean concentration with time and space is assumed to be described by the convection–diffusion equation

$$\frac{\partial \langle c\rangle_{\text{cell}}}{\partial t} + \langle v\rangle^f \frac{\partial \langle c\rangle_{\text{cell}}}{\partial x} = D_{xx}\frac{\partial^2 \langle c\rangle_{\text{cell}}}{\partial x^2} + D_{yy}\frac{\partial^2 \langle c\rangle_{\text{cell}}}{\partial y^2} + Q\delta(x)\delta(y)\delta(t) \tag{15}$$

where $\langle c\rangle_{\text{cell}}$ is the average concentration at point (x, y) at time t, $\langle v\rangle^f$ the interstitial velocity of the flow in the x direction, Q the source intensity, and D_{xx} and D_{yy} the longitudinal and lateral dispersion coefficients.

This equation is true if and only if the principal dispersion tensor direction coincides with the flow direction. According to Amaral-Souto (1993) this condition is satisfied as soon as $Pe_p > 200$ in regular geometries, and $Pe_p > 100$ in random arrangements, where Pe_p is the particulate Péclet number introduced by Carbonell and Whitaker (1983), defined by

$$Pe_p = \frac{\langle v\rangle^f d_p}{\mathscr{D}} \frac{\varepsilon}{1-\varepsilon} \tag{16}$$

and d_p is the equivalent particle diameter defined by the equation $d_p = 6/A_v$, where A_v is the specific area of the medium; ε is the porous medium porosity.

For an instantaneous source located at the origin in a porous medium assumed to be of infinite extent, the solution of eq. (15) is given by

$$\langle c\rangle_{\text{cell}}(x, y, t) = \frac{Q}{4\pi t\sqrt{D_{xx}D_{yy}}} \times \exp\left[-\frac{(x - \langle v\rangle^f t)^2}{4D_{xx}t} - \frac{y^2}{4D_{yy}t}\right] \tag{17}$$

where the concentration at infinite distance from the injection point is equal to zero at all times. Here, Q is the source intensity, namely the mass quantity injected at $t = 0$ per unit length.

In the experiments, lateral spreading is not significant and does not reach the lateral walls of the medium. The medium can therefore be considered as infinite in the Oy direction. By monitoring the time variation of the tracer concentration up to steady state, the longitudinal dispersion coefficient can be estimated. It is evaluated by comparing the time profiles of mean concentration measured at $y = 0$ with the solution (17) of eq. (15):

$$\langle c\rangle_{\text{cell}}(x_0, y = 0, t) = \frac{A}{t}\exp\left[-\frac{(x_0 - \langle v\rangle^f t)^2}{4D_{xx}t}\right] \tag{18}$$

where x_0 is the axial position of the observation point, which is assumed to be accurately known.

This method serves to identify three parameters:

- longitudinal dispersion coefficient D_{xx}
- velocity $\langle v\rangle^f$, i.e. the interstitial velocity. It is derived from the syringe-pump delivery rate. The procedure can be validated by comparing the experimental determination with the experimental value by curve fitting.
- $A = \dfrac{Q}{4\pi\sqrt{D_{xx}D_{yy}}}$.

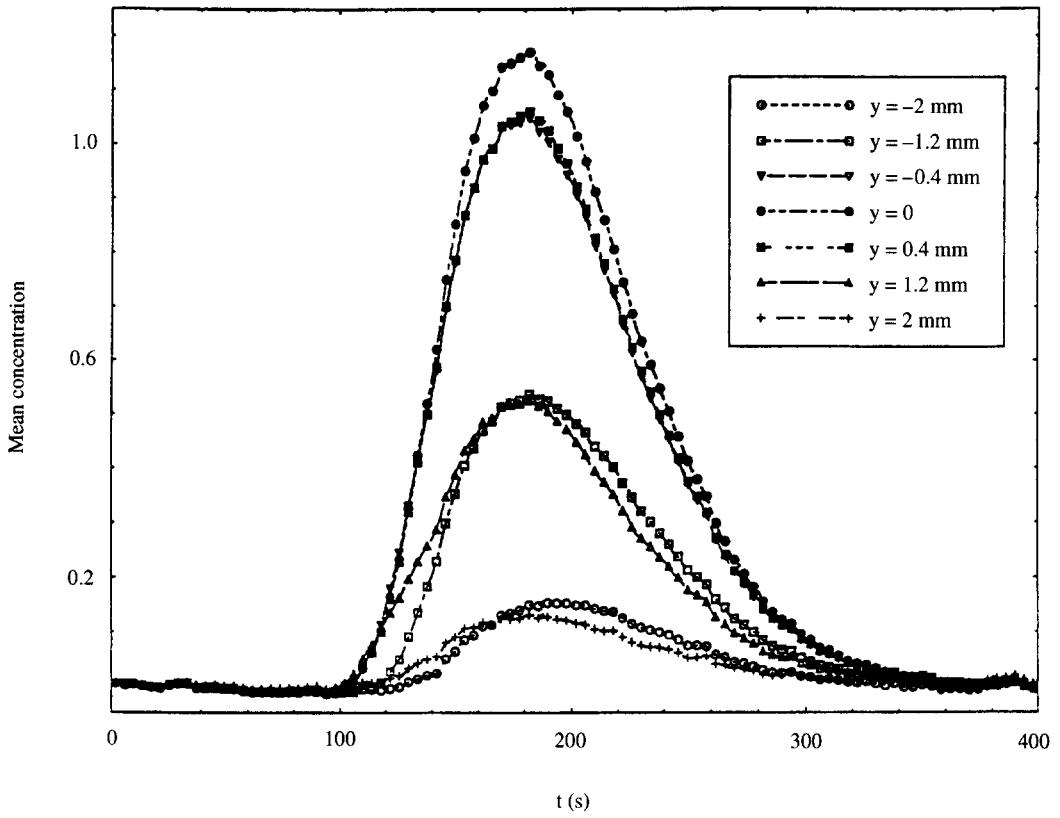

Fig. 6. Concentration vs time for various transverse positions.

The simplex method is used to fit the experimental curves with eq. (18) using the least-squares distance. Wakao (1982) discussed the parameter estimation techniques. He demonstrated that, of all the analytical techniques (moment method, transfer function fitting, Fourier analysis, and others) curve fitting in the time domain is the most reliable.

Determination of point $(x_0, 0)$

As shown by eq. (17), identification of the longitudinal dispersion coefficient is much simpler at the points $(x_0, 0)$, i.e. on the streamline flowing through the injection point. The experimental procedure involves moving the averaging volume (taken as unit cell) continuously perpendicular to the flow. The concentration is plotted vs time in Fig. 6 for various transverse positions. Point $y = 0$ corresponds to the position with the maximum concentration.

EXPERIMENTAL RESULTS

Model validity

The validity of eq. (18) was checked for the porous media investigated. Figures 7 and 8 show the two typical situations. The first case (Fig. 7) is obtained for a measurement point close to the injection point, corresponding to $(x/d_p)/Pe_p = 0.045$. The solid line corresponds to the model [eq. (18)] with an interstitial velocity calculated to coincide with the time at which the maximum concentration is reached. This curve does not fit the experimental results (dots). The head of the curve is slightly steeper, and a long time tail is observed. This behaviour is characteristic of transient dispersion: diffusion time at pore scale $d_p^2/\mathscr{D}$ is longer than convection time $x/\langle v\rangle^f$. By contrast (Fig. 8 corresponding to $(x/d_p)/Pe_p = 0.13$), good agreement is obtained between the experimental data and the best fit of the model. The difference between the identified and experimentally measured velocities is less than a few per cent. All the results presented in this study use measurements taken far enough from the injection point to satisfy the foregoing constraint.

In-line cylinders: mean flow at 0°

This medium is analysed for two directions of the mean flow: 0 and 26°. The mean flow direction is located with respect to the test column wall. The medium [Fig. 2(a)] comprises 29 unit cells in width and 140 lengthwise. Each cell is 0.8 mm square. The mean cylinder diameter is 0.51 mm, and the porosity is 0.68. To determine the longitudinal dispersion coefficient, the variation in concentration with time is analysed at $y = 0$. The maximum concentration occurs at time $t_{max} = x/\langle v\rangle^f$. Figure 9 shows a plot of the mean concentrations for five different values of x. The mean flow velocity given by the syringe pump is 3.34×10^{-4} m/s. The velocity determined from the relation t_{max} vs x in Fig. 10 is 3.28×10^{-4} m/s, in good agreement with theory. The curves in Fig. 9 are then fit by

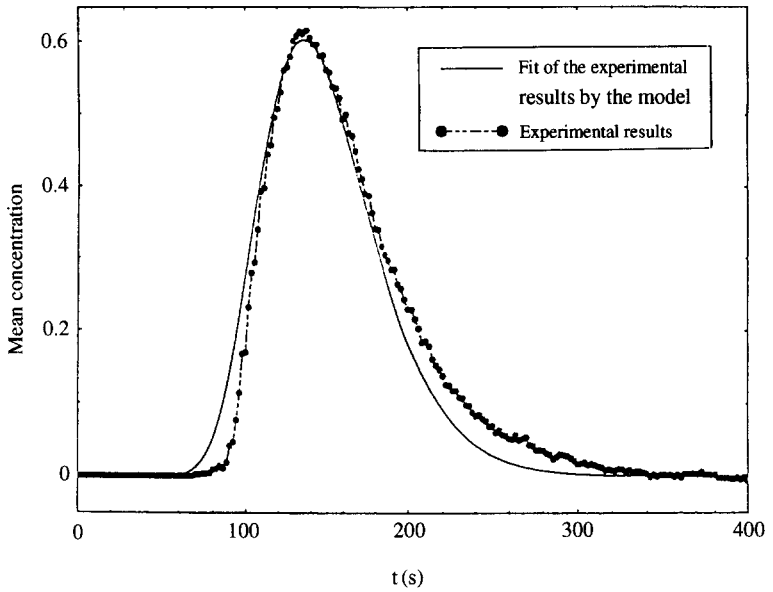

Fig. 7. Concentration vs time at $x = 39 \times 10^{-3}$ m for $\langle v \rangle^f = 2.7 \times 10^{-4}$ m/s: transient case.

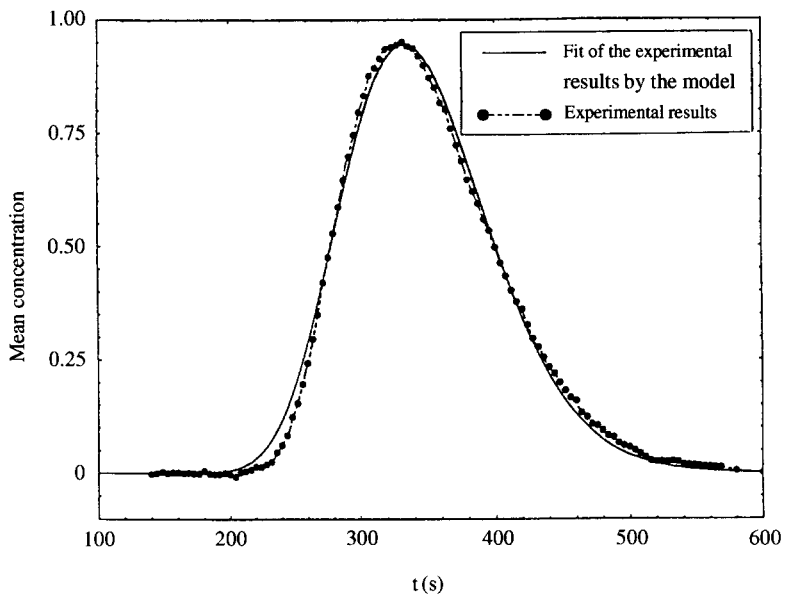

Fig. 8. Concentration vs time at $x = 79 \times 10^{-3}$ m for $\langle v \rangle^f = 2.4 \times 10^{-4}$ m/s.

the function (18). The particulate Péclet number is 842. The longitudinal dispersion coefficient is 2.11×10^{-7} m^2/s $\pm$ 3% for the five different curves. The same experiments were carried out for various velocities. The ratio $D_{xx}/\mathscr{D}$ versus Pe_p between 200 and 1200 is plotted in Fig. 11. The molecular diffusion coefficient $\mathscr{D}$ is 4×10^{-10} m^2/s for methylene blue in water.

In-line cylinders: mean flow at 26°

The unit cell is positioned in the test column so that the mean flow direction is at 26° with respect to the unit cell axis. The medium [Fig. 2(b)] comprises 14 cylinders in width and 300 lengthwise corresponding approximately to 112 unit cells. The mean cylinder diameter is 0.508 mm and the void fraction 0.68. The identification procedure for the longitudinal dispersion coefficient is identical to the one described above. The results are given in Fig. 11.

Random distributed medium

This experimental medium is the same as the one used by Amaral-Souto (1993) to compute the dispersion tensor [Fig. 2(c)]. The unit cell contains 36 cylinders 0.5 mm in diameter. Each cell is a 5 mm square. The medium comprises 5 unit cells widthwise and 22 lengthwise. The void fraction is 0.578. Figure 12

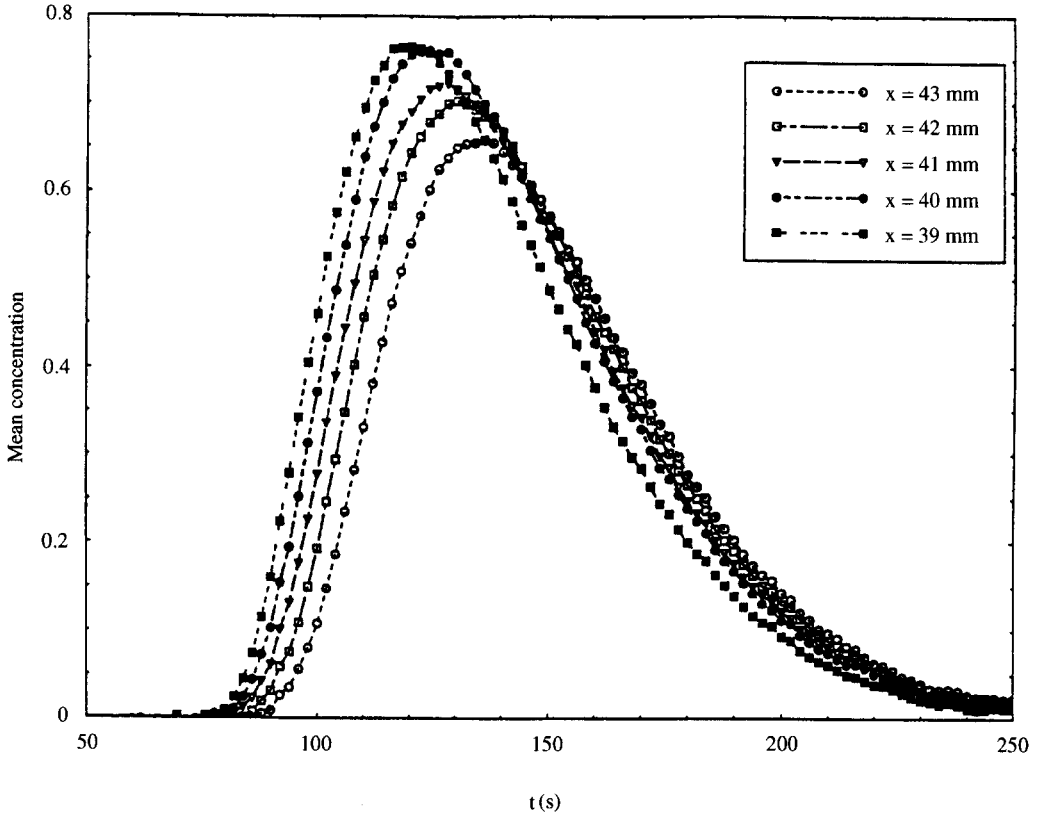

Fig. 9. Concentration vs time for various axial positions: $\langle v \rangle^f = 3.34 \times 10^{-4}$ m/s.

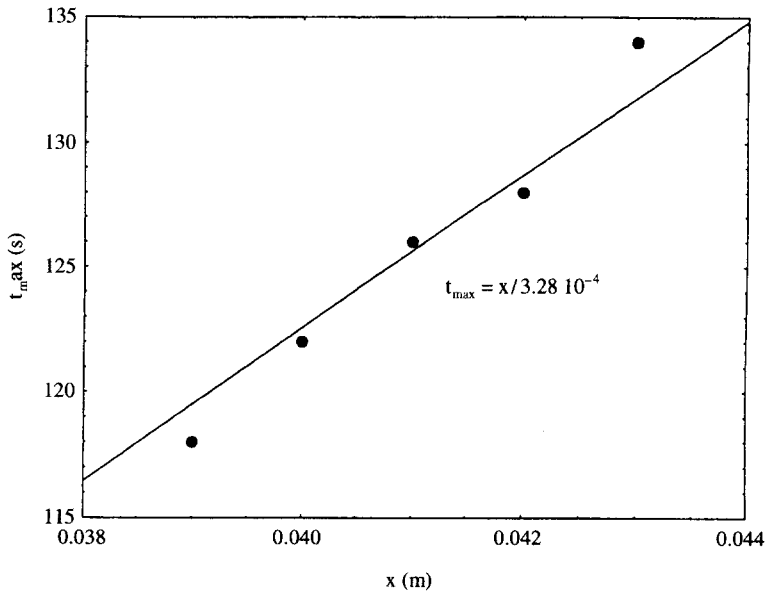

Fig. 10. Time for maximum concentration vs axial positions.

shows the variation of $D_{xx}/\mathscr{D}$ vs Pe_p. In the range of particulate Péclet numbers from 400 to 1900, the value of $D_{xx}/\mathscr{D}$ is two to three times higher for disordered cells, in accordance with intuitive knowledge.

COMPARISON BETWEEN THEORY AND EXPERIMENT

In-line cylinders ($\theta = 0°$)

The first configuration analysed concerned in-line circular cylinders with an average fluid velocity parallel to the line linking the centres of the cylinders ($\theta = 0°$).

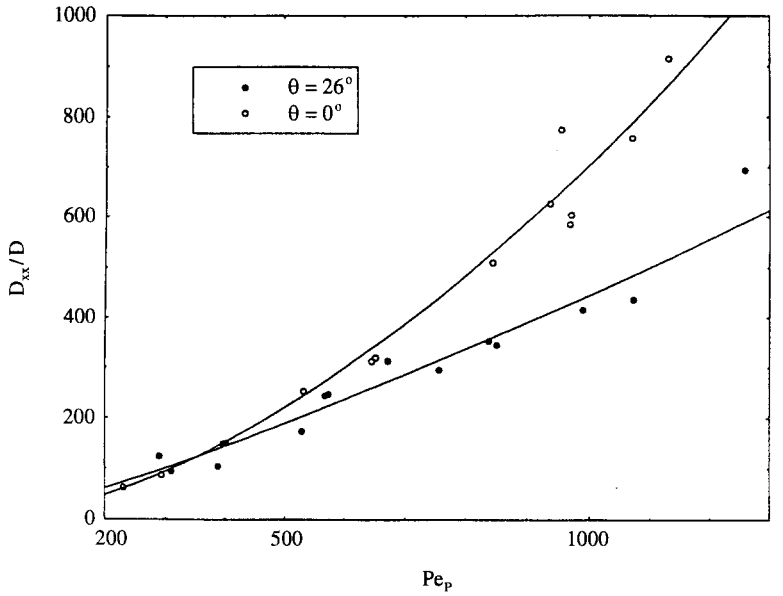

Fig. 11. Experimental variations of $D_{xx}/\mathscr{D}$ vs Pe_p for in-line cylinders. Mean flow at 0° and 26°.

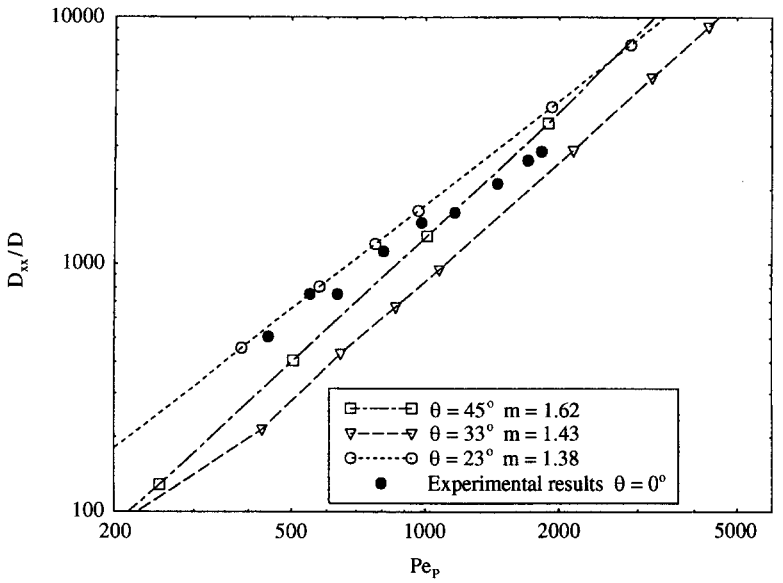

Fig. 12. Random distributed medium. $D_{xx}/\mathscr{D}$ vs Pe_p. Comparison between experimental results for $\theta = 0°$ with numerical results from Amaral Souto for $\theta = 23$, 33 and 45°.

Much numerical data can be found in the literature for comparison with the experimental results, including Eidsath *et al.* (1983) (in-line circular and square cylinders, $\theta = 0°$, $\varepsilon = 0.37$); Edwards *et al.* (1991) (in-line circular cylinders, $\theta = 0°$, $\varepsilon = 0.60$); Salles *et al.* (1993) (in-line circular cylinders, $\theta = 0°$, $\varepsilon = 0.59$); Amaral Souto (1993) (in-line square cylinders, with $\theta = 0°$ and staggered square cylinders with $\theta = 45°$, $\varepsilon = 0.64$, i.e. an in-line array of square cylinders rotated 45°). Figure 13 compares between these numerical results and the experimental results obtained for the longitudinal dispersion coefficient $D_{xx}/\mathscr{D}$ vs particulate Péclet number Pe_p.

A number of differences are apparent, both among the numerical values themselves and between the numerical and experimental results. The numerical data for the in-line array of circular cylinders or square cylinders are very close for all authors. Nevertheless, the experimental points do not fit these curves but, surprisingly, are very close to the numerical results for in-line array of square cylinders rotated 45°. For the high particulate Péclet numbers investigated ($Pe_p >$ 100), the points lie nearly in a straight line on a log–log plot, with an almost identical slope but with different ordinates at the origin. This behaviour is commonly described by analysing the relation of

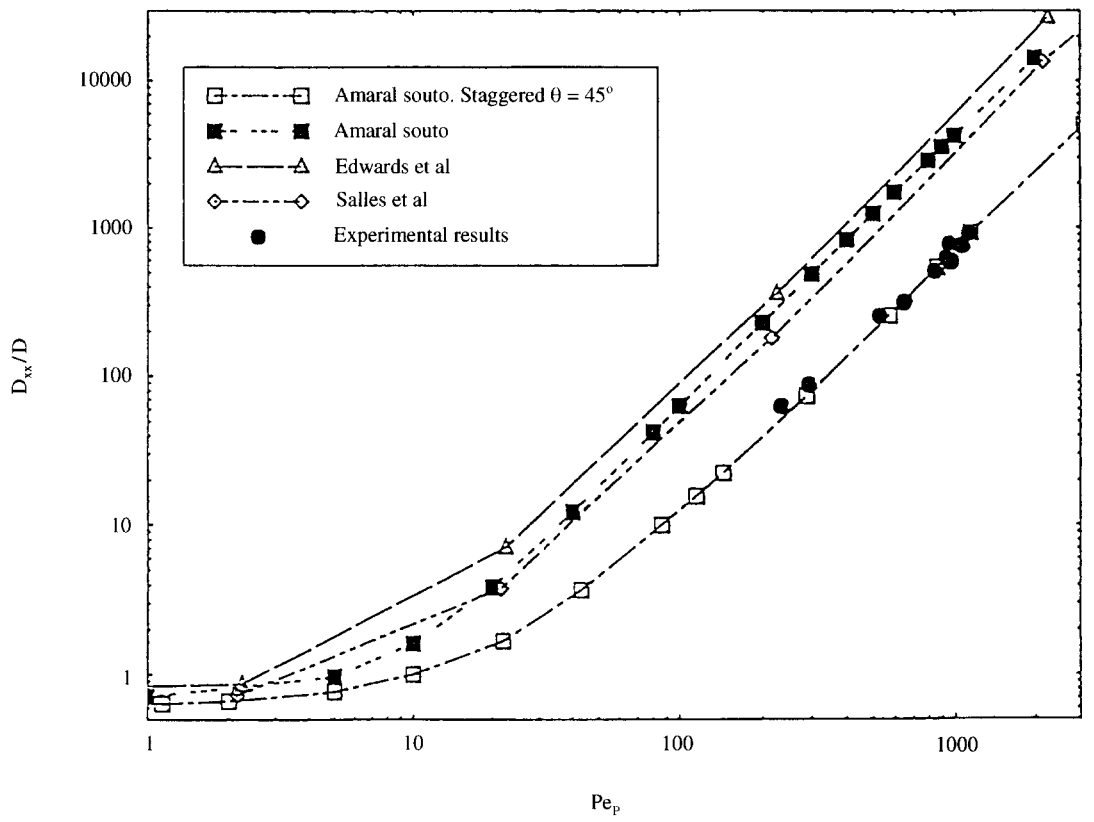

Fig. 13. Variations of $D_{xx}/\mathscr{D}$ vs Pe_p. In-line cylinders. Mean flow at 0°. Comparison between various numerical results and experimental results.

$D_{xx}/\mathscr{D}$ vs Pe_p (for high enough Pe_p) in the form

$$\frac{D_{xx}}{\mathscr{D}} = A\,Pe_p^m. \tag{19}$$

In Fig. 11, the solid line corresponds to the linear adjustment for m in log–log coordinates. This adjustment was obtained with a correlation coefficient in the range 0.97–0.99. The values of the exponent m are given in Table 1. These lie in the range $1.67 < m < 1.83$. Note, however, that these values are significantly less than 2, which is the standard value observed for Taylor dispersion through a tube.

Several factors may explain this discrepancy between theoretical and experimental results. First, since the values for m are far from 2, the uncertainty in the molecular diffusion coefficient $\mathscr{D}$ may modify the experimental curves. The theory is also valid for a two-dimensional situation. In fact, the experiment is necessarily three-dimensional, owing to the two plates where the needles are fixed. Moreover, while the periodicity of the medium may be quite satisfactory, small defects are unavoidable in the form of the cylinders [Salles *et al.* (1993) discussed the significant effects of small defects in the array]. Finally, some uncertainties can be expected due to the solute injection process (regarded as a Dirac distribution both in time and space).

Table 1. Values of m for in-line cylinders: numerical data from Salles *et al.* (1993), Amaral Souto (1993) and Edwards *et al.* (1991)

θ		m
0°	Edwards *et al.* ($\varepsilon = 0.6$)	1.79
0°	Salles *et al.* ($\varepsilon = 0.59$)	1.78
0°	Amaral Souto ($\varepsilon = 0.64$)	1.83
45°	Amaral Souto ($\varepsilon = 0.64$) staggered	1.71
0°	Experimental results ($\varepsilon = 0.68$)	1.67
30°	Salles *et al.* ($\varepsilon = 0.59$)	1.43
22.5°	Amaral Souto ($\varepsilon = 0.64$)	1.31
26°	Experimental results ($\varepsilon = 0.68$)	1.24

However, owing to the discrepancies between numerical results for the same geometry, agreement between experimental and theoretical results concerning the exponent m can be regarded as satisfactory.

In-line cylinders ($\theta = 26°$)

Varying the angle θ between the average fluid flow and the line linking the centres of the cylinders entails fabricating a new medium each time. Only one case was tested: $\theta = 26°$. Few results are available in the literature for such a case. To the best of our knowledge, only Salles *et al.* (1993) (for circular cylinders) and

Amaral Souto (1993) (for square cylinders) have computed the dispersion tensor by varying the angle θ.

In accordance with the foregoing comments for the case $\theta = 0°$, the comparison between the theoretical and the experimental results is restricted to the values of the exponent m defined by eq. (19). The values of m are given in Table 1. All the results agree, showing a very significant influence of the direction of the average fluid velocity. The values of m lie in the range $1.2 < m < 1.4$, which is considerably less than 2. Both the numerical and experimental values of m, and the effective values of $D_{xx}/\mathscr{D}$, are significantly less than those measured at $\theta = 0°$ in the same range of Péclet numbers.

Random periodic medium

The results are shown in Figure 12 for $\theta = 0°$, and are compared with the numerical results of Amaral Souto (1993), who used the same arrangement, but for square cyliders and for $\theta = 23$, 33 and 45°. For random periodic porous media, the influence of the value of the angle θ has been investigated elsewhere (Amaral Souto, 1993). Generally, the value of the angle θ has a weak influence on the dispersion tensor. In the case of the medium studied, the numerical values of the longitudinal dispersion tensor are given in Fig. 12 for $\theta = 23$, 33 and 45°. The experimental values are slightly lower, but in good agreement. The exponent value is $m = 1.2$ for the experimental values, and $m = 1.38$ for the numerical results, for $\theta = 23°$. It is worth noting that the experimental value $m = 1.2$ corresponds to the value commonly assumed by various experimenters (Pfannkuch, 1963; Ebach and White, 1958; Carberry and Bretton, 1958; Edwards and Richardson, 1968; Blackwell, 1959; Rifai *et al.*, 1956; Han *et al.*, 1985) for 'real', in fact random, porous media.

COMPARISON WITH ANALYSIS OF KOCH *ET AL.*

Koch *et al.* (1989) questioned the relevance of periodic porous media for investigating the dispersion of 'real' or random porous media. Based on an approximate solution of the theory for low solid volume fractions, they concluded that if the unit cell is symmetrical with respect to its two orthogonal axes (as for in-line cylinders), for high Péclet numbers, then the longitudinal (or transverse) dispersion coefficient exhibits two different behaviours: If the average velocity is not perpendicular to an axis of the lattice (i.e. if $\tan\theta$ is not rational), the dispersion coefficients become independent of Pe_p and proportional to the molecular diffusion coefficient $\mathscr{D}$. In the opposite case, (i.e. if $\tan\theta$ is rational), the quantity $D/\mathscr{D}$ must vary as Pe_p^2 for both the longitudinal and transverse dispersion coefficients. Intuitively, the particular character of dispersion through periodic porous media is linked to the correlation of the flow field, which occurs due to the spatial frequency of the medium. In fact, the question is: Is the molecular diffusion sufficient to introduce a random character comparable with the behaviour of 'real' porous media?

Contrary to Koch *et al.* (1989), simultaneously for the experimental and numerical values, for the in-line case with $\theta = 0°$, the value of the exponent m is close to but significantly less than 2. When $\theta = 26°$, neither the numerical nor the experimental results are in agreement with the theory of Koch *et al.* Their arguments appear to be oversimplified, and their conclusions concerning the relevance of periodic porous media therefore have to be reconsidered.

CONCLUSION

The experimental system appears to be highly promising. The technique yields reproducible results with good accuracy. Agreement between experimental and numerical results is very satisfactory.

For in-line cylinders, the experimental results clearly demonstrated the effect of the flow direction on the dispersion coefficients. By comparison with numerical results, it is possible to appreciate the influence of the particle shape in regular arrangements. Considering the influence of these two geometric characteristics of the media, periodic porous media formed with a regular unit cell do not serve as good model for describing dispersion in real porous media.

A single experimental report is not enough to conclude concerning the random periodic medium, but is rather encouraging. Considering the numerical results obtained by Amaral Souto (1993) for 20 arrangements of square cylinders in the unit cell, the average value of m is equal to 1.59 ± 0.20 with no significant variation with the mean flow direction. Experimental and numerical results appear to indicate that, in despite of its periodic character, this type of medium can describe the behaviour of homogeneous porous media if the unit cell is sufficiently large to represent the porous media structure.

The numerical method is suitable only for periodic porous media. The experimental method can now be used to study dispersion in random two-dimensional porous media, and can probably be extended to three-dimensional porous media.

NOTATION

c	local solute concentration
$\langle c\rangle^f$	intrinsic average concentration
$\langle c\rangle_{\text{cell}}$	average concentration over a unit cell
$\mathscr{D}$	molecular diffusion coefficient
d_p	equivalent particle diameter
D_{xx}	longitudinal dispersion coefficient
D_{yy}	transversal dispersion coefficient
m	exponent of Péclet number defined in eq. (19)
Pe_p	particulate Péclet number
Q	source intensity
t	time from start of injection tracer
$\mathbf{v}$	local velocity of the fluid
$\langle v\rangle^f$	intrinsic average velocity
x, y	space variables in the plane of study

Greek letters

$\delta(t)$	Dirac delta function for time variable
$\delta(x)$	Dirac delta function for space variable
ε	porous medium porosity
θ	direction of the mean flow

REFERENCES

Amaral Souto, H. P. (1993) Diffusion–dispersion en milieu poreux: étude numérique du tenseur de dispersion pour quelques arrangements périodiques bidimensionnels "ordonnés" et "désordonnés". Thesis de l'Institut National Polytechnique de Lorraine, Nancy, France.

Amaral Souto, H. P. and Moyne, C. (1996a) Dispersion in two-dimensional periodic porous media. Part I: hydrodynamics. *Phys. Fluids* (submitted).

Amaral Souto, H. P. and Moyne, C. (1996b) Dispersion in two-dimensional periodic porous media. Part II: dispersion. *Phys. Fluids* (submitted).

André, J. C. and Corbel, S. (1994) *Stéréopholithograhie laser*. Polytechnica ed.

Aris, R. (1956) On the dispersion of a solute in a fluid flow through a tube. *Proc. Roy. Soc.* **A235**, 67–77.

Baveye P. and Sposito, G. (1984) The operational significance of the continuum hypothesis in the theory of water movement through soils and aquifers. *Water Resources Res.* **20**, 521–530.

Blackwell, R. J., Rayne, J. R. and Terry, W. M. (1959) Factors influencing the efficiency of miscible displacement. *Petroleum Trans. AIME* **216**, 1–8.

Brenner, H. (1980) Dispersion resulting from flow through spatially periodic porous media. *Phil. Trans. Roy. Soc.* **297**, 81–133.

Carberry, J. J. and Bretton, R. H. (1958) Axial dispersion of mass in flow through fixed beds. *A.I.Ch.E. J.* **4**, 367–375.

Carbonell, R. G. and Whitaker, S. (1983) Dispersion in pulsed system II. *Chem. Engng Sci.* **38**(11), 1795–1802.

Corbel, S., Allanic, A. L., Schaeffer, P. and André, J. C. (1994) Computer-aided manufacture of three dimensional objects by laser space resolved photopolymerisation. *J. Intelligent Robotic Systems* **9**, 301–312.

Ebach, E. A. and White, R. R. (1958) Mixing of fluids flowing through beds of packed solids. *A.I.Ch.E. J.* **4**, 161–169.

Edwards, D. A., Shapiro, M., Brenner, H. and Shapira, M. (1991) Dispersion of inerte solutes in spatially periodic two dimensional model porous media. *Transport Porous Media* **6**, 337–358.

Edwards, M. F. and Richardson, J. F. (1968) Gas dispersion in packed beds. *Chem. Engng Sci.* **23**, 109.

Eidsath, A., Carbonell, R. G., Whitaker, S. and Herrmann, L. R. (1983) Dispersion in pulsed systems III. Comparison between theory and experiments for packed beds. *Chem. Engng Sci.* **38**(11), 1803–1816.

Gunn, D. J. and Pryce, C. (1969) Dispersion in packed beds. *Trans. Instn Chem. Engrs* **47**, 341–350.

Han, N. W., Bhakta, J. and Carbonell, R. G. (1985) Longitudinal and lateral dispersion in packed beds: effect of column length and particle size distribution. *A.I.Ch.E. J.* **31**, 277–288.

Horn, F. J. M. (1971) Calculation of dispersion coefficients by means of moments. *A.I.Ch.E. J.* **17**, 613–620.

Karrer, P., Corbel, S., André, J. C. and Lougnot, D. J. (1992) Shrinkage effects in photopolymerizable resins containing filling agents: application to stereophotolithography. *J. Polym. Sci.* **30**, 2715–23.

Koch, D. L. and Brady, J. F. (1985) Dispersion in fixed beds. *J. Fluid Mech.* **154**, 399–427.

Koch, D. L., Cox, R. G., Brenner, H. and Brady, J. F. (1989) The effect of order on dispersion in porous media. *J. Fluid Mech.* **200**, 173–188.

Mei, C. C. (1992) Method of homogeneization applied to dispersion in porous media. *Transport Porous Media* **9**, 261–274.

Pfannkuch, H. O. (1963) Contribution à l'Etude des Déplacements de Fluides miscibles dans un Milieu Poreux. *Revue l'Institut Français Pétrole* **XVIII**, 215–270.

Rifai, M., Kaufman, W. J. and Todd, D. K. (1956) Dispersion in Laminar flow through porous media. Sanitary Eng. Res. Lab. Rpt. No. 3, IER, Series 90, Berkeley.

Rubinstein, J. and Mauri, R. (1986) Dispersion and convection in porous media. *SIAM J. Appl. Math.* **46**, 1018.

Salles, J., Thovert, J. F., Delannay, R., Prevors, L., Auriault, J. L. and Adler, P. (1993) Taylor dispersion in porous media. Determination of the dispersion tensor. *Phys. Fluids* A **5**, 2348–2376.

Wakao, N. and Kaguei, S. (1982) *Heat and Mass Transfer in Packed Beds*, p. 364. Gordon and Breach, New York.